

A Modeling Study of Ozone Production Rates During the Summers of 2002 and 2006

James Godowitch^{1*}, Golam Sarwar¹, and Shuang Chen²

¹ National Exposure Research Laboratory, US EPA, Research Triangle Park, NC

² Dept. of Meteorology, Pennsylvania State University, University Park, PA

1.0 INTRODUCTION

The production and accumulation of tropospheric ozone (O_3) are governed by atmospheric physical and chemical processes. While physical processes determine the transport, dispersion, and removal of existing O_3 , the formation of additional O_3 occurs through complex interactions of numerous photochemical reactions involving a variety of volatile organic compounds (VOCs) and nitrogen oxides (NO_x) that are emitted from anthropogenic and natural sources.

In this study, the temporal evolution and spatial variability of the ozone production rate are examined during the summer periods of 2002 and 2006 with the Community Multiscale Air Quality (CMAQ) model (Byun and Schere, 2006). Additionally, since the model simulations were performed for a summer period before and another period after the US EPA's NO_x SIP Call Rule, the impact on ozone production from significant NO_x emission reductions at major point sources was also be assessed.

2. STUDY DESCRIPTION

2.1 Modeling Details and Simulations

The CMAQv50 model was applied with the Carbon Bond 2005 (CB05) chemical mechanism. Simulations spanned the period from June 1 through August 31 in 2002 and 2006 with a 10-day spin-up period prior to each starting date. Boundary conditions were provided by the GEOS-Chem global model concentrations based on a 2006 annual simulation.

The modeling domain (299 x 459) extended beyond the continental US and also contained large parts of Canada and Mexico with a 12 km horizontal grid cell size. The vertical structure contained 35 layers with the thickness of layer 1 reduced to ~20 m.

Meteorological fields for both periods were generated by the Weather Research and Forecasting (WRFv3.3) model. WRF was applied with an updated four-dimensional data technique (Gilliam et al., 2012), which utilized available observed wind, temperature, and moisture profiles to provide improved 3-D modeled meteorological parameter fields. The CMAQ Meteorology-Chemistry Interface Processor (MCIP v4.1) was used to reformat the WRF output into input data sets containing the hourly 2-D and 3-D meteorological fields for the CMAQ simulations. Specific options applied in the WRF model simulations are described in Gilliam et al. (2012).

The emission data sets were generated by the Sparse Matrix Operator Kernel Emissions (SMOKE) processing system. Anthropogenic emissions from the EPA 2002 and 2005 National Emissions Inventories (NEI) were used to generate surface and minor point source emissions, however, hourly pollutant emissions of major point sources were specified from the Continuous Emissions Monitoring System (CEMS) data sets. Natural surface emissions of NO_x , isoprene, and other biogenic VOC species were computed by the Biogenic Emissions Inventory System (BEISv3.14). Gridded on-road vehicle emissions for these model simulations were obtained from the MOBILE6 model using projections of vehicle-miles-traveled (VMT) and fleet factors for reference counties within each state for each summer period.

2.2 Method for Ozone Production Rates

The total ozone production rate ($P(O_3)$) was computed from eqn. (1) using the model output concentrations. $P(O_3)$ is determined from the sum of the chemical reactions of the hydroperoxy radical (HO_2) and organic peroxy radical species (RO_2) with nitric oxide (NO) in the CB05 chemical mechanism as noted by Chen et al. (2010).

$$P(O_3) = k_{HO_2}[HO_2][NO] + \sum k_i[RO_{2,i}][NO] \quad (1)$$

Hourly gridded $P(O_3)$ values for layer 1 for each day during each simulation period were determined from the sum of CB05 reactions involving NO with HO_2 and RO_2 species. Chen et al. (2010) found

* Corresponding author: J. Godowitch, US EPA, NERL, E243-04, RTP, NC 27711. phone: 919-541-4802, email: godowitch.james@epa.gov

differences in $P(O_3)$ among chemical mechanisms with CB05 and the SAPRC07 results being very close as well as higher than others in their study. The reaction rate coefficients (k_i) in eqn (1) were also adjusted by the surface air pressure and ambient temperature of each grid cell in layer 1. It must be highlighted that these $P(O_3)$ values represent total or instantaneous ozone production values since loss reactions are not considered. These $P(O_3)$ values are expected to be generally higher than the chemistry rate term obtained from the process analysis (PA) option which represents a net value involving both ozone production and loss reactions.

3. SELECTED RESULTS

3.1 Spatial Variation of $P(O_3)$

The spatial variability in the mean maximum $P(O_3)$ values in the modeling domain for summer 2002 is displayed in Figure 1. These maxima coincided with high photochemical activity during the early afternoon hours. It is apparent that the highest $P(O_3)$ values exist within and near to major urban areas across the US. In fact, the mean maximum values in several cities exceeded 25 ppb/hr, while the mean maximum values in rural areas were generally from 5-8 ppb/hr.

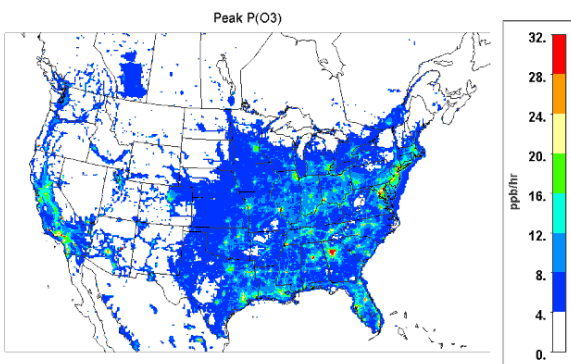


Fig. 1. Spatial distribution of mean maximum $P(O_3)$ values in the modeling domain during summer 2002.

Of particular interest is the extent of decline in $P(O_3)$ values from 2002 to 2006 as a consequence of the substantial NO_x emission reductions during 2003-04 associated with the implementation of controls due to the NO_x SIP Call Rule on major point sources. In addition, there was also a gradual year-to-year decrease in mobile source NO_x emissions evident from the MOBILE 6 model. In fact, Godowitch et al. (2011) reported modeled weekday urban morning NO_x concentrations decreased by close to 15% from 2002 to 2006.

The percentage change in the mean maximum $P(O_3)$ values between these summer 2002 and 2006 periods is depicted in Figure 2. The largest declines in $P(O_3)$ values exceeding $\approx -30\%$ are found in the Ohio River and Tennessee River valley regions, which are attributable to the large reductions in major power plant NO_x emissions in these areas. There were also notable declines in mean maximum $P(O_3)$ within the northeast corridor cities from Washington, DC to Boston, portions of New England and the mid-Atlantic states, as well as southern Canada. On the other hand, there were increases in $P(O_3)$ of 15-25% in some areas of the southern states and as well as coastal California.

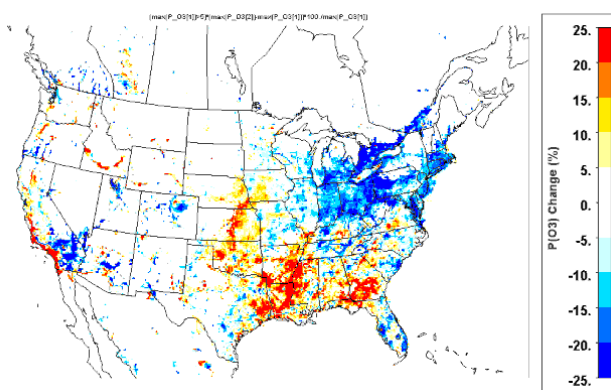


Fig. 2. Change (%) in the mean maximum $P(O_3)$ in the model domain from summer 2002 to 2006. Note: results are shown only where $P(O_3) > 5$ ppb/hr.

3.2 Temporal Behavior of O_3 Production

The temporal variation of $P(O_3)$ over the daytime period was also analyzed based on all model grids cells containing AQS urban sites and at rural CASTNET site locations. The results displayed in Figure 3 are hourly averaged values from all days during both periods. Clearly, mean $P(O_3)$ exhibits a large daytime variation with maximum values in the early afternoon hours. Due to an abundance of anthropogenic NO_x and VOCs, urban results are higher by a factor of 4 or more than those found at the rural CASTNET site locations. Additionally, there is a noticeable decrease in mean $P(O_3)$ of close to 15% at both sets of monitoring sites.

The time variation of $P(O_3)$ in several large cities exhibiting the highest mean values during summer 2002 are shown in Figure 4. Mean $P(O_3)$ values in these urban areas exceeded 25 ppb/hr with Atlanta exhibiting the highest mean value. Although differences existed in the time of the maximum

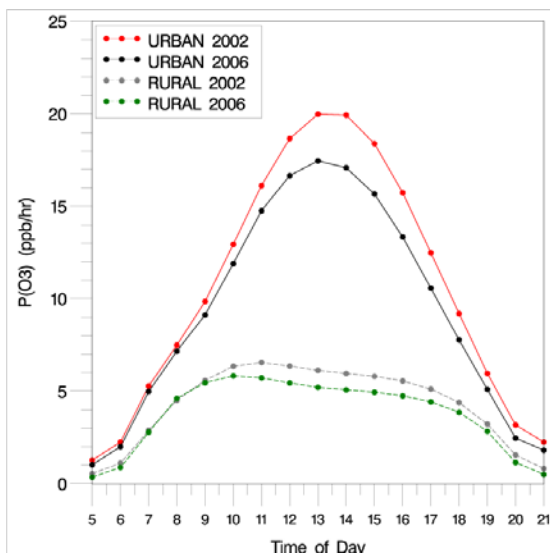


Fig. 3. Time variation of $P(O_3)$ at AQS urban and rural CASTNET sites from summer 2002 and 2006 periods.

$P(O_3)$ value, it is apparent that the highest values occurred during an early afternoon hour followed by a continuous decline toward zero near sunset. Additionally, magnitudes of $P(O_3)$ during the rise in the morning hours appear to be relatively similar, while greater differences in $P(O_3)$ are evident among these urban areas during the afternoon period.

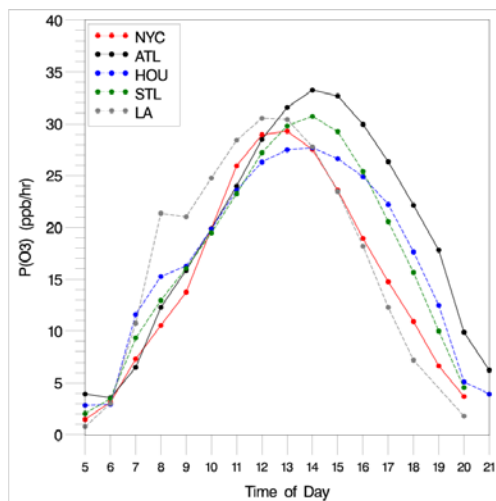


Fig. 4. Daytime variation of mean $P(O_3)$ in five cities from summer 2002.

The cumulative distributions of daily maximum $P(O_3)$ values from these summer periods in several urban areas (ex., Figure 5) were also analyzed to identify possible changes in ozone production rates due to the NO_x emission changes. Results at the

90th percentile of the $P(O_3)$ distributions for summer 2002 and 2006 indicated notable differences in various urban areas. For example, in New York City (NYC, Fig. 5a) the maximum $P(O_3)$ at the 90th percentile dropped from 61.0 ppb/hr to 42.8 ppb/hr corresponding to a 29.8% decrease. Changes in maximum $P(O_3)$ values at the 90th percentile varied greatly among the urban areas. A decrease of 15.3% was found in Washington, DC, while slight increases of 7.7 and 4.6% occurred in Atlanta and Houston (Fig. 5b), respectively. There was no change in maximum $P(O_3)$ in St. Louis, while Los Angeles showed a small decrease of 5.5%. These results concur with the spatial pattern exhibited in Figure 2, which revealed the most notable decreases in the Ohio River Valley (ORV) and northeastern areas. At the upper portion of the ORV, $P(O_3)$ in Pittsburgh decreased by 8.7%. Godowitch et al. (2011) also showed that the notable decreases in maximum 8-h O_3 coincided with these same areas.

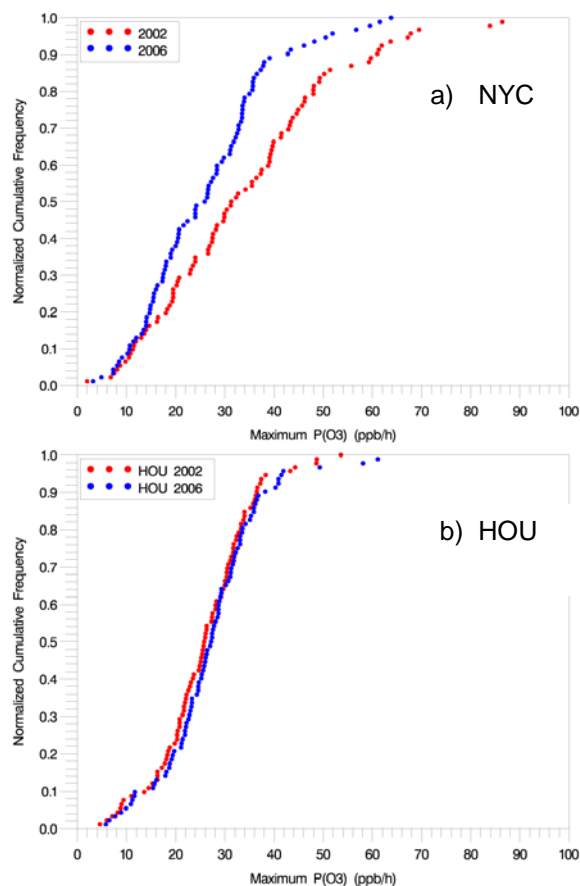


Fig. 5. Cumulative distributions of $P(O_3)$ for a) New York City (NYC) and b) Houston, TX (HOU) during summer 2002 and 2006.

The day-to-day variation of $P(O_3)$, based on values from the urban AQS and rural CASTNET sites in the eastern US during the summer 2002 period, is displayed in Figure 6. Large day-to-day

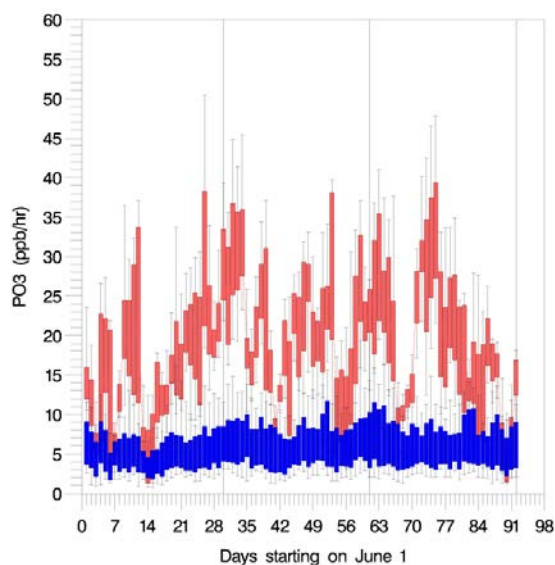


Fig. 6. Daily variation of mid-day $P(O_3)$ at urban AQS sites (red) and at rural CASTNET sites (blue) during the summer 2002 period. Boxes span the 25th-75th percentiles and whiskers extend from the 10th-90th percentiles based on the sites from each network.

variations in $P(O_3)$ are certainly evident in the set of urban locations with mean values ranging from 5 to > 30 ppb/h. $P(O_3)$ values at rural CASTNET sites are considerably lower and exhibit much less daily variability and differences among the rural sites are smaller on each day than those at urban locations.

4. SUMMARY

Ozone production rates, based on CMAQ modeled concentrations using key photochemical reactions of NO with HO_2 and RO_2 species in the CB05 chemical mechanism, were computed for two different summer periods. Results showed large spatial variability across the modeling domain. As anticipated, the highest values were found in major urban areas. Maximum values typically occurred during an early afternoon hour, however, substantial day-to-day variations in the magnitudes of the maximum $P(O_3)$ occurred among urban locations, while considerably smaller daily differences were apparent in rural locations. The notable declines in $P(O_3)$ between these summer periods existed in areas where large NO_x emission reductions had taken place, namely, the Ohio River

and the Tennessee River valley regions, as well as in many urban areas along the northeast corridor.

DISCLAIMER

Although this work was reviewed by EPA and approved for publication, it may not necessarily reflect official Agency policy.

REFERENCES

- Byun, D., Schere, K.L., 2006: Review of the governing equations, computational algorithms, and other components of the Models-3 Community Multiscale Air Quality (CMAQ) modeling system. *Applied Mechanics Reviews*, 59, 51-77.
- Chen, S., et al., 2010: A comparison of chemical mechanisms based on TRAMP 2006 field data. *Atmos. Environ.*, 44, 4116-4125.
- Gilliam, R.C., J.M. Godowitch, S.T. Rao, 2012: Improving the horizontal transport in the lower troposphere with four dimensional data assimilation. *Atmos. Environ.*, 53, 186-201.
- Godowitch, J.M., G.A. Pouliot, S.T. Rao, 2011: Assessing multi-year changes in modeled and observed urban NO_x concentrations from a dynamic evaluation perspective. *Atmos. Environ.*, 44, 2894-2901.